Journal of Catalysis **210,** 53–66 (2002)
doi:10.1006/jcat.2002.3682

Mechanistic Studies on the Oxidative Dehydrogenation of Methanol over Polycrystalline Silver Using the Temporal-Analysis-of-Products Approach

Andre C. van Veen, Olaf Hinrichsen, and Martin Muhler[1]

Ruhr-Universität Bochum, Lehrstuhl für Technische Chemie, D-44780 Bochum, Germany

Received November 26, 2001; revised March 14, 2002; accepted April 25, 2002

The temporal-analysis-of-products approach was used to study the mechanism of the oxidative dehydrogenation of methanol over an unsupported polycrystalline silver catalyst. Pulse experiments revealed a distinct influence of the state of the silver surface on the adsorption of oxygen and on reactivity toward methanol. The surface-embedded oxygen species O_γ, which is stable at high temperatures, was found to provide a highly selective reaction pathway for the oxidation of methanol to formaldehyde above 550 K. A comparison of the pulse responses of formaldehyde, water, and hydrogen to methanol pulses showed that water is a primary gas-phase product and that only small amounts of hydrogen are formed. Furthermore, it was found that the O_γ species is not active in the oxidation of hydrogen or carbon monoxide. In contrast, the much more active adsorbed oxygen species O_α was observed to be involved in the nonselective deep oxidation of methanol at lower temperatures, yielding carbon dioxide at high coverages. However, at low coverages O_α also causes the selective formation of formaldehyde.

Key Words: **silver; methanol; oxygen; oxidative dehydrogenation; temporal analysis of products (TAP).**

1. INTRODUCTION

Formaldehyde is a major product of industrial organic chemistry, which produces, worldwide, about 5×10^6 tons per year (1, 2). A main production process is the selective oxidation of methanol over a thin layer of unsupported silver grains under adiabatic conditions feeding a methanol–air mixture (approximately 1 : 1 molar ratio) diluted with steam in the temperature range of 850–923 K at atmospheric pressure. The reaction temperature depends on the amount of excess methanol in the mixture. Higher temperatures, up to 1000 K, result in a nearly full conversion and a yield of formaldehyde of about 90% (3, 4). Alternatively, formaldehyde is produced over a mixed iron- and molybdenum-containing oxidic catalyst (Mo : Fe molar ratio of 1.5 : 2.0) in a multitubular fixed-bed reactor at about 673 K. This process employs a high excess of air, resulting in a nearly full conversion of methanol and a yield of formaldehyde of about 90% [4].

Despite numerous research efforts in recent years (5–9), there is ongoing debate in the literature about the reaction mechanism over silver. Controversial opinions exist on the function and importance of different oxygen species. Wachs and Madix (5) proposed a detailed reaction mechanism based on model studies performed on the Ag(110) single-crystal surface. It was suggested that surface-bound atomic oxygen creates the active site for the dissociative adsorption of methanol, yielding the methoxy species as an adsorbed intermediate, which decomposes to formaldehyde and hydrogen. Based on studies on polycrystalline silver, Millar *et al.* (8) concluded that methanol reacted with subsurface oxygen species located in the topmost layer to produce subsurface hydroxyl species, which subsequently formed water. However, it is generally accepted that the interaction of oxygen with a silver catalyst at different temperatures leads to the formation of different oxygen species (9–14). In addition, an oxygen treatment at atmospheric pressure and at high temperatures leads to pronounced morphological changes in the catalyst (15–17).

Recent studies employing spectroscopic and temperature-programmed techniques led to the identification of three different atomic oxygen species above room temperature, termed O_α, O_β, and O_γ (9, 11, 12). O_α desorbs at about 600 K and represents chemisorbed, surface-bound atomic oxygen, which can also dissolve in the bulk. The bulk-dissolved atomic oxygen species is termed O_β. The nucleophilic species O_γ is embedded in the uppermost layer of silver atoms and exhibits a remarkable thermal stability, with a desorption temperature of about 900 K. O_β diffuses through high-indexed crystalline structures and along grain boundaries. Thus, O_γ is the intermediate state where O_β segregates from the bulk to the surface via interstitial diffusion. The high desorption temperature implies that O_γ plays an important role in the oxidation of methanol. Previous studies devoted to mechanistic investigations into the importance of O_γ used the temperature-programmed surface reaction (TPSR) of methanol with samples exposing different oxygen species simultaneously (18) or were carried out under atmospheric pressure with a methanol–oxygen

[1] To whom correspondence should be addressed. E-mail: muhler@techem.ruhr-uni-bochum.de.

0021-9517/02 $35.00

reactant cofeed (9). As the adsorption of gas-phase oxygen during the latter experiments leads to the formation of O_α, there are at present no data available reflecting the reactivity of O_γ without interference by O_α. Furthermore, hints of the occurrence of homogeneous gas-phase reactions were found (9), which, in turn, might cause difficulties in data interpretation. In addition, steady-state methanol oxidation is known to induce large morphological changes of the catalyst, resulting in an even more complicated interpretation of the obtained results.

Thus, we chose a different approach and studied the silver-catalyzed oxidation of methanol using the temporal-analysis-of-products (TAP) system (19). The use of small reactant pulses under high-vacuum conditions allowed us to probe the catalytic properties of different surface states virtually nondestructively. Therefore, it was possible to obtain information on the reactivity of different oxygen species without interference by other species. Suitable pretreatment procedures had to be applied in order to obtain the individual oxygen species. Furthermore, the applied high-vacuum conditions were found to suppress gas-phase reactions and the thermal decomposition of the selective product formaldehyde.

Based on the results of pulse and flow experiments a deeper insight into the reaction mechanism was achieved. Furthermore, different functions of the oxygen species were identified. Finally, a detailed reaction scheme based on the obtained results is presented.

2. EXPERIMENTAL

Materials

All experiments were carried out using 0.5 g of electrolytically prepared silver particles with a diameter of less than 0.5 mm, supplied by Degussa. Oxygen (99.999%), carbon monoxide (99.997%), and neon (99.999%) were obtained from Messer Griesheim, and hydrogen (99.9999%) was purchased from Air Products. These gases were used without further purification. In addition, ultrahigh-purity water-free methanol (99.8%, Aldrich) and demineralized water were used after applying a few freeze–pump–thaw cycles and the removal of air traces by several evacuation cycles. Formaldehyde was freshly obtained by thermal decomposition of *n*-hydroxymethylbenzamide (98%, Lancaster) and was used diluted in neon as reference gas mixture at higher temperatures ($T > 350$ K) to avoid oligomerization.

TAP Setup

All experiments were conducted in a temporal-analysis-of-products setup in which the catalyst is usually operated under high-vacuum conditions. As the setup was equipped with a movable high-pressure sealing assembly (TAP-1b), a conventional reactor operation made it possible to apply pretreatment procedures at atmospheric pressure. Special care had to be taken to eliminate wall reactions and adsorption phenomena within the highly oxidized reactor after applying *in situ* pretreatments. Therefore, a modified passivated reactor was used as described elsewhere (20). Dosing of reactants from the gas feed system incorporated the use of high-speed pulsed or continuously opening valves. A quantitative, submillisecond time-resolved detection of pulse responses was accomplished by the use of a calibrated quadrupole mass spectrometer (UTI 100C). As a benefit of the low pressure (1.1×10^{-9} mbar) only small background signals had to be subtracted during analysis to give true signal responses for all components. Therefore, a very sensitive detection of small numbers of molecules was possible.

In order to calibrate the various reactants and products analyzed in this work, mass spectra of individual binary mixtures of pure gases in neon were obtained from continuous flow scan experiments through the reactor filled with an inert quartz bed. From these spectra, calibration coefficients were calculated for each gas. Neon was monitored at $m/e = 20$, oxygen at $m/e = 32$, methanol at $m/e = 31$, formaldehyde at $m/e = 30$, CO_2 at $m/e = 44$, CO at $m/e = 28$, H_2O at $m/e = 18$, and H_2 at $m/e = 2$. Since the mass spectrum of methanol also contains minor fragments at $m/e = 30$ and 32, these contributions were subtracted to obtain the true signal responses of formaldehyde and oxygen, respectively. Thus, taking the fragmentation patterns and the calibration factors into account, the molar flux of the molecules leaving the reactor during the pulse experiments is reported relative to the internal standard neon (flux/a.u.).

The calibration allowed us to calculate the detected molar amounts for reactants $R(n_{R,e})$ and products $P(n_{P,e})$ in reference to the detected amount of the internal standard component neon (n_I). Furthermore, the ratio between the amount of pulsed reactants and neon ($n_{R,0}/n_I$) is known from the partial pressures used in reactant mixtures, assuming ideal gases. Hence, it is possible to calculate the pulsed reactant amounts for each experiment, which, in turn, allowed us to determine reactant conversions (X_R) and product yields (Y_P):

$$X_R = \frac{n_{R,0} - n_{R,e}}{n_{R,0}} = 1 - \frac{n_{R,e}/n_I}{n_{R,0}/n_I}, \qquad [1]$$

$$Y_P = -\frac{\nu_R}{\nu_P} \cdot \frac{n_{P,e}}{n_{R,0}} = -\frac{\nu_R}{\nu_P} \cdot \frac{n_{P,e}/n_I}{n_{R,0}/n_I}. \qquad [2]$$

The calculation of yields requires the assumption of a formal reaction equation, where ν_R and ν_P are the stoichiometric coefficients for the considered reactant and product. Despite the fact that product formation within some reported reaction steps are shown to occur via different routes, it is assumed throughout this work that the formation of hydrogen and water exclusively takes place by

partial dehydrogenation and oxidative dehydrogenation of methanol to formaldehyde, respectively, to enable a simplified comparison of the results.

The pulse size is calculated from pressure drop measurements within a known volume of the feed system for several pulses. Furthermore, information on the interaction of reactants with the catalyst can be derived from the pulse responses. A simple quantitative comparison of pulse shapes is accomplished by calculating the ratio between the measured average residence time and the average residence time of nonadsorbing molecules (19), termed normalized average residence time ($t_a/t_{a,I}$) in the following.

Pretreatment of the Catalyst

In order to obtain the oxygen-treated surface state, the catalyst was oxidized under severe conditions. The reactor was loaded with 0.5 g silver and transferred into high vacuum. After 1 h of heating at 373 K, the high-pressure sealing assembly was applied to the reactor and 1150 mbar pure oxygen were dosed with a continuous flow of approximately 0.5 ml min^{-1}(STP). The oxidation was carried out by heating the reactor with 10 K min^{-1} up to 923 K. After holding the sample at this temperature for one night in oxygen, it was cooled to 723 K and kept in a vacuum for 1 h to remove any adsorbed species. In this way, the carbonaceous impurities in the Ag grains were removed as CO_2, the bulk of the Ag grains was saturated with dissolved atomic oxygen (O_β), and the high-temperature stable O_γ species embedded in the topmost surface layer was created. The above pretreatment was chosen in reference to spectroscopic studies on the Ag(111) surface by Bao *et al.* [21], in which the authors found the formation of a very high coverage of O_γ using a comparable pretreatment.

Oxygen-free samples were prepared by temperature-programmed reduction of oxygen-treated catalysts in a 1 : 10 methanol-in-neon mixture. The sample was heated at 5 K min^{-1} from room temperature to 888 K in a continuous flow of about 0.5 ml min^{-1} (STP) streaming toward the vacuum applied at the reactor exit. After reduction of the sample for about 30 min at maximum temperature, the reactor was subsequently cooled to room temperature at 20 K min^{-1} in the reduction mixture. In this way, significant differences in specific surface areas between oxygen-treated and oxygen-free samples caused by sintering were avoided.

A surface with a high coverage of O_α was obtained by adsorption of gas-phase oxygen on an oxygen-free catalyst at lower temperature. Usually, 1000 mbar pure oxygen was dosed at a temperature of 473 K for more than 1 h.

Characterization

Specific surface areas were determined by the BET method using a Quantachrome Autosorb 1C setup. The adsorption of nitrogen (99.9999%) or krypton (99.998%) supplied by Messer Griesheim was carried out at 77 K. Results were calculated based on cross-sectional areas of 16.2×10^{-20} m^2 (nitrogen) and 20.5×10^{-20} m^2 (krypton).

Scanning electron microscopic (SEM) micrographs were taken with a LEO 1530 SEM setup. Sintering caused the formation of loosely adhering porous aggregates during the high-temperature pretreatment of the silver grains. In order to obtain representative images for the whole fixed bed, the grains were separated again by gentle crushing. No coating of the grains had to be applied, as they were electrically conducting and fixed onto the sample holders by graphite sticking pads.

Temperature-programmed desorption experiments with the oxygen-treated catalyst were carried out within the TAP setup. A small continuous flow of neon (approximately 0.5 ml min^{-1}(STP)) was fed to the reactor, and the experiment was started by raising the temperature linearly with different heating ramps. A maximum time resolution of 1 min was possible for the analysis of the effluent gas, as data acquisition for different gas components was accomplished by recording complete mass scans up to $m/e = 50$. Due to the addition of Ne as internal standard, it was possible to obtain the amount of desorbed oxygen by integrating the TPD traces versus time.

3. RESULTS

Characterization

The pretreatment of the catalyst involved the application of high temperatures, which may lead to a lowering of the specific surface area by sintering. Therefore, fresh and used catalyst samples were characterized by BET measurements. In good agreement with previous studies by Bao and Deng (6) and Rigas *et al.* (22) a specific surface area of 0.19 ± 0.04 m^2 g^{-1} was found by nitrogen physisorption on fresh samples (8.73 g). However, used samples had a much lower surface area and meaningful results for the limited amount of Ag sample could only be obtained by krypton adsorption. Using 3.18 g obtained by combining the Ag samples of several experiments, a specific surface area of 5.2×10^{-3} m^2 g^{-1} was determined, corresponding to a mean particle diameter of 0.1 mm. Based on an average value of 1.15×10^{19} Ag surface atoms m^{-2}, a 6×10^{16} Ag surface atoms g^{-1} is derived.

Figure 1 shows SEM micrographs of a fresh silver sample and of samples after the application of different pretreatment procedures. Pronounced changes in catalyst morphology are visible. Figure 1a is an image of the fresh catalyst. The surface consists of broad flat areas, and a few grooves, probably caused by mechanical stress, are visible. In contrast, the surface of the oxygen-treated catalyst shown in Fig. 1b exhibits a completely different morphology. A pronounced faceting of the surface took place during the high-temperature pretreatment in oxygen. Planar facets with an

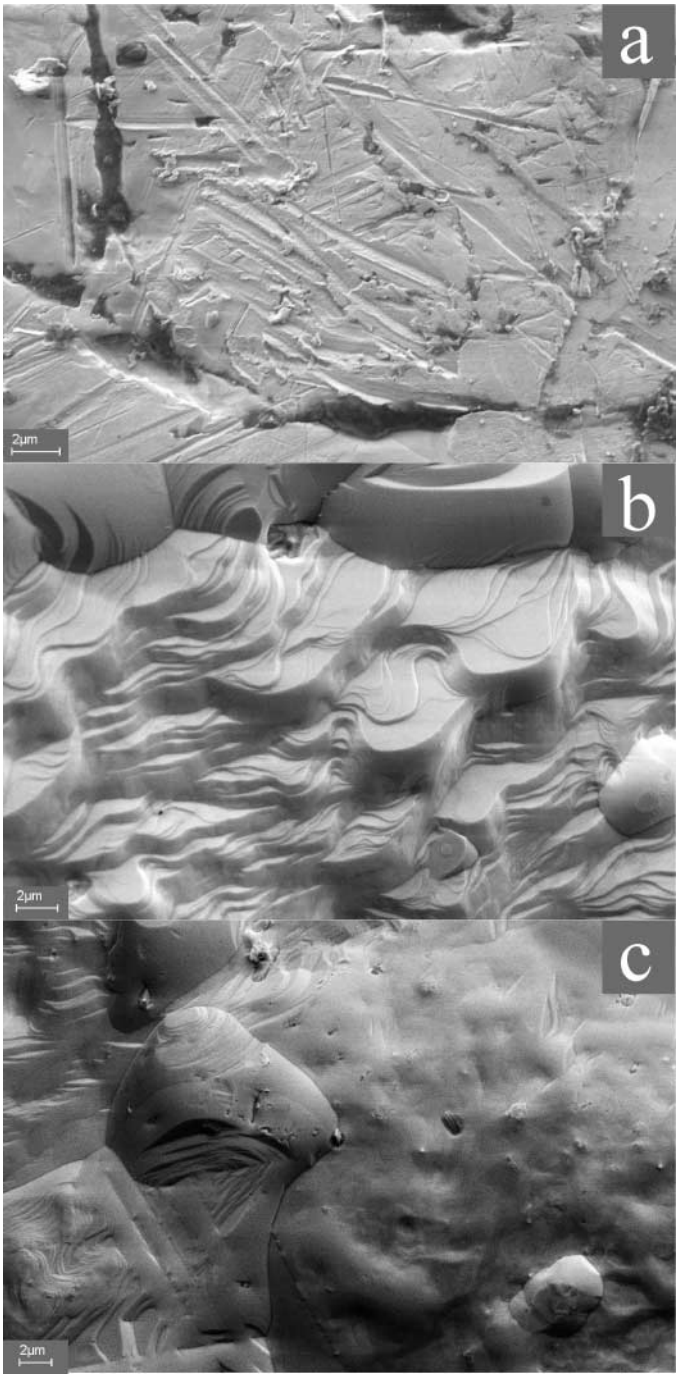

FIG. 1. SEM micrographs of the silver grains after different pretreatments. (a) Fresh catalyst; (b) oxygen-treated catalyst; (c) oxygen-free catalyst.

average diameter of about 2 μm appeared, forming a perfect terrace-and-step structure. Macroscopically, the corrugated surfaces appear dull. Figure 1c shows a micrograph of the oxygen-free catalyst obtained by reduction with methanol. It is clearly visible that the reduction caused a destruction of all facets. Therefore, the surface appears to be much smoother in comparison to the oxygen-treated state. However, in contrast to the fresh sample, the surface is not completely flat and fragments of the hill-and-valley morphology formed during the previous oxygen treatment are still visible.

O_2 TPD of the Oxygen-Treated Catalyst

In contrast to the usual oxygen-treatment procedure, the oxygen atmosphere was not removed during cooling to permit further adsorption of oxygen. After reaching room temperature, a complete flushing of gas-phase oxygen was accomplished by evacuation for 1 h. Figure 2 shows the oxygen desorption spectra of the oxygen-treated catalyst obtained with heating ramps of 5, 10, and 15 K min^{-1}. Oxygen desorption starts at temperatures above 750 K, and the desorption maxima are detected at about 900 K. The symmetric shape of the desorption signal and the characteristic desorption temperature indicate the pronounced formation of O_γ during the oxidizing pretreatment at atmospheric pressure. Furthermore, no significant oxygen desorption is observed at about 600 K, within the experimental detection limit, which would indicate the presence of O_α (10, 23–27). As the sample was cooled to room temperature in oxygen, which should have caused the formation of O_α on clean silver surfaces, it can be concluded that the formation of O_α was suppressed on the O_γ-containing facets. Thus, the chosen pretreatment procedure exclusively causes the formation of O_γ as active oxygen species within the surface region. Furthermore, the onset of oxygen desorption at 750 K requires restricting experiments with a well-defined O_γ-containing state of the catalyst to a maximum temperature of about 700 K.

As expected from desorption without significant readsorption, the TPD peak heights correlate well with the heating rates. The integration yields, on average, 0.09 μmol O_2 g^{-1}, which corresponds to roughly 10^{17} oxygen

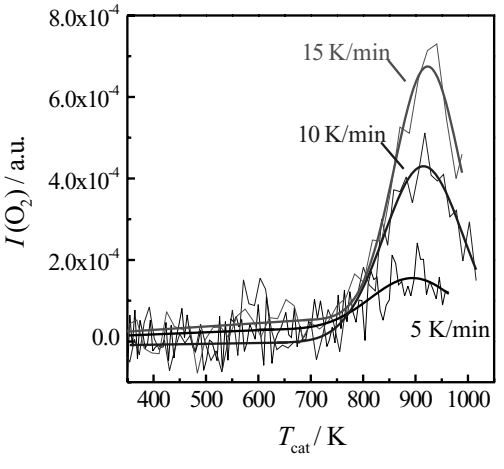

FIG. 2. O_2 TPD spectra obtained with the oxygen-treated catalyst using heating ramps of 5, 10, and 15 K min^{-1}.

atoms g^{-1}, available in the surface region in the oxygen-treated state of the catalyst. This value is in reasonable agreement with the number of Ag surface atoms derived from the Kr BET measurement, taking the experimental errors into account.

The Interaction of the Catalyst with Oxygen

The interaction of oxygen with the catalyst as a function of the pretreatment was further investigated by pulse experiments. Approximately $2–3 \times 10^{14}$ molecules of a 1 : 3 oxygen-in-neon mixture were pulsed through the catalyst bed. Figure 3a displays the response signals as a flux of oxygen molecules leaving the reactor versus time for an experiment over the oxygen-free catalyst at different temperatures. A comparison of the pulse responses indicates that the detected pulse size, and, in turn, the oxygen amount leaving the reactor, decreases with increasing catalyst temperature despite the fact that the pulsed amount remains constant. Furthermore, the response signals are sharpened, which leads to a shift of the signal maxima to shorter times

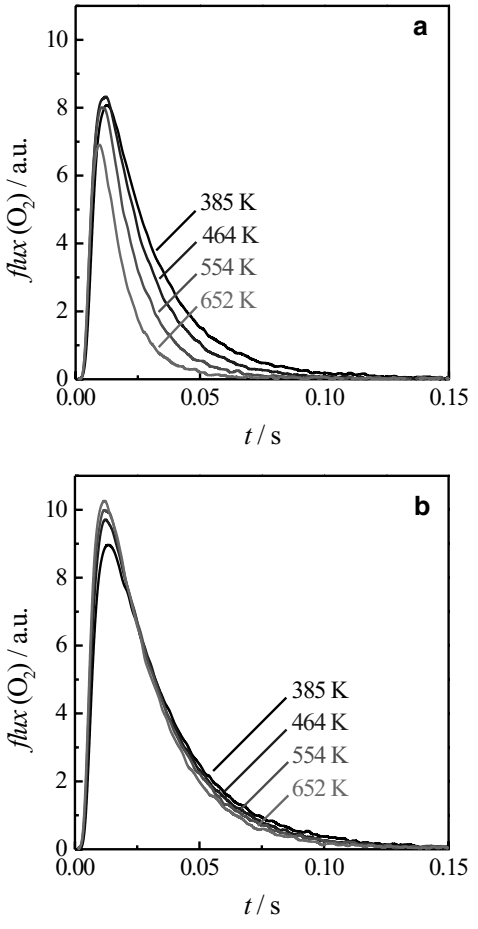

FIG. 3. Oxygen responses for pulses of 2×10^{14} molecules of a 1 : 3 oxygen-in-neon mixture in the temperature range between 380 and 660 K. (a) Oxygen-free catalyst; (b) oxygen-treated catalyst.

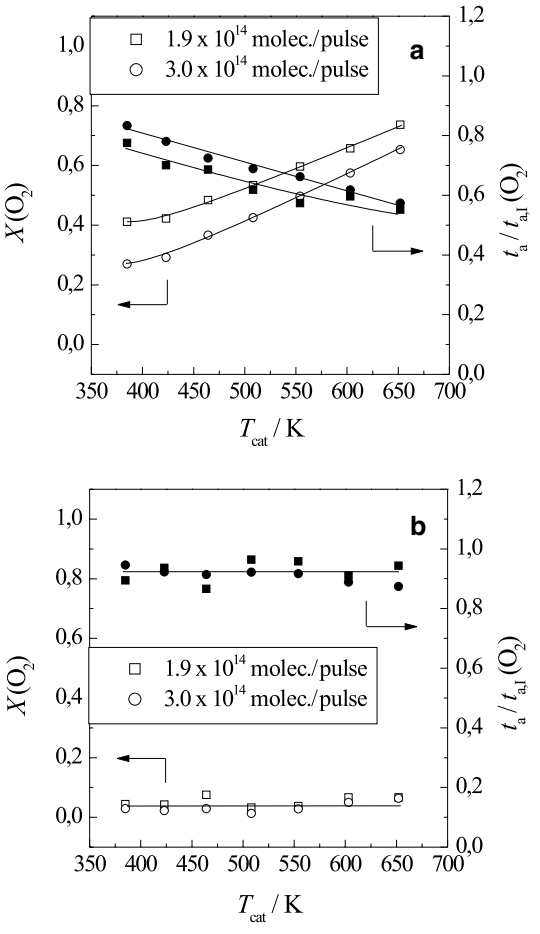

FIG. 4. Oxygen conversion and normalized average residence time for pulses of $1.9–3.0 \times 10^{14}$ molecules of a 1 : 3 oxygen-in-neon mixture in the temperature range between 380 and 660 K. (a) Oxygen-free catalyst; (b) oxygen-treated catalyst.

with increasing catalyst temperature. This observation indicates increasing oxygen consumption at higher temperatures, as will be discussed later.

The response signals for a similar experiment over an oxygen-treated catalyst are shown in Fig. 3b. In contrast to the responses obtained by experiments over the oxygen-free catalyst, no pronounced temperature dependence of the signals is observed. Furthermore, all detected pulses have equal sizes and show comparable shapes. The small shift of the peak position toward shorter times at higher temperature can be attributed to the square-root temperature dependence of the mass transport by Knudsen diffusion.

The results of these pulse experiments can also be expressed in terms of oxygen conversion (X) and the normalized average residence time ($t_a/t_{a,I}$). Therefore, Fig. 4 summarizes the results along with those of further experiments with different pulse sizes. Figure 4a displays the results of experiments over the oxygen-free catalyst at different temperatures. The oxygen conversion increases with rising

temperature, but no formation of oxidized products such as carbon monoxide, carbon dioxide, or water is observed during the experiments. These findings thus indicate an activated, irreversible adsorption of oxygen within the short time scale of the pulse experiment, instead of a conversion of oxygen to products. The observed temperature dependence arises from the fact that the number of oxygen molecules with the required amount of energy for an activated adsorption increases with rising temperature. Furthermore, the normalized average residence time remains below 1.0 and is observed to decrease at higher temperatures, reflecting a sharpening of pulse responses. This behavior originates from an irreversible adsorption of especially those oxygen molecules with a long residence time and therefore higher adsorption probability. It must be noted that the mass transport only occurs via Knudsen diffusion of less than 10^{15} molecules per pulse, according to Fick's second law. Thus, the inlet pulse shape, which can be described by a Dirac delta function, ideally is broadened asymmetrically. Hence, the preferred adsorption of these molecules leads to an increasing deficiency of detected oxygen molecules in the reactor effluent at longer times.

The calculated conversions and normalized average residence times for comparable experiments with different pulse sizes show only small differences. Hence it is safe to exclude a pronounced channeling of reactants during experiments with the lower pulse size despite the fact that the catalyst sample exposes only a very small number of adsorption sites.

Results from similar experiments over an oxygen-treated catalyst are shown in Fig. 4b. No significant oxygen conversion is observed within the investigated temperature range. Therefore, an (irreversible) adsorption of oxygen can be excluded. Furthermore, as no conversion occurs, the temperature dependence of the normalized average residence time allows us to obtain information on reversible adsorption processes. A constant value of about 1.0 is found for $t_a/t_{a,I}$ at all temperatures, indicating that also no reversible interaction of oxygen takes place with the oxygen-treated catalyst.

The Interaction of the Oxygen-Treated Catalyst with Carbon Monoxide and Hydrogen

Pulse experiments with carbon monoxide over an oxygen-treated catalyst were conducted to elucidate the reducibility of O_γ. Figure 5 displays the results in terms of carbon monoxide conversion (X) and normalized average residence time ($t_a/t_{a,I}$) at different catalyst temperatures. Under all applied conditions no significant carbon monoxide conversion was obtained. Therefore, a reaction of O_γ with carbon monoxide can be excluded. In addition, the ratio between the measured average residence time and the average residence time of nonadsorbing molecules remains almost constant during all experiments, amounting to

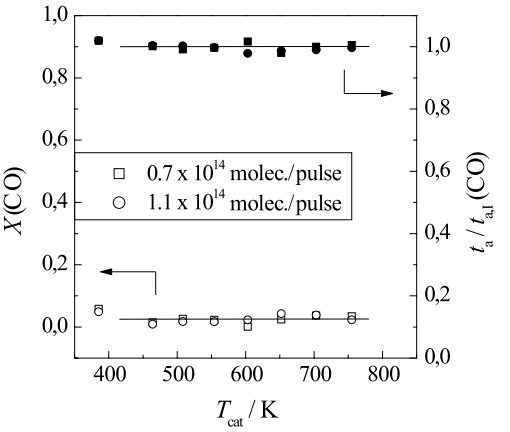

FIG. 5. Carbon monoxide conversion and normalized average residence time for pulses of $0.7–1.1 \times 10^{14}$ molecules of a 1 : 3 carbon monoxide-in-neon mixture in the temperature range between 380 and 750 K over an oxygen-treated catalyst.

1.0 and showing no temperature dependence. Thus, a pronounced reversible interaction of carbon monoxide with O_γ can be excluded, too.

Figure 6 shows the results of pulse experiments with a 1 : 3 hydrogen-in-neon mixture over the oxygen-treated catalyst at different catalyst temperatures. No pronounced temperature dependence of the hydrogen conversion is observable. Nevertheless, as reported previously (28) an insufficient pumping speed of light molecules probably causes experimental problems for the detection of hydrogen transients. Therefore, the detected amount of hydrogen is typically overestimated in comparison to the amount of the well-pumped internal-standard-component neon, which, in turn, leads to a calculation of lowered conversions on the basis of continuous-flow calibrations. In contrast to the observed behavior, a pronounced temperature dependence

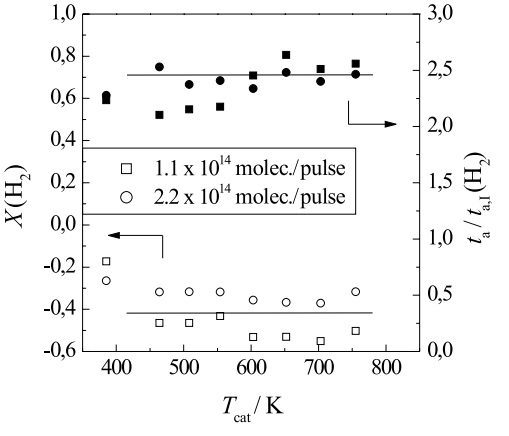

FIG. 6. Hydrogen conversion and normalized average residence time for pulses of $1.1–2.2 \times 10^{14}$ molecules of a 1 : 3 hydrogen-in-neon mixture in the temperature range between 380 and 750 K over an oxygen-treated catalyst.

of the conversion has to be expected if a chemical reaction occurs. Thus, despite of the calculated value of approximately −0.4 no true conversion is obtained and no reaction of hydrogen with O_γ takes place. In addition, the normalized average residence time ($t_a/t_{a,I}$) shows no temperature dependence, for which a value of approximately 2.5 is obtained for all experiments. This result is in good agreement with the assumption of a broadened signal caused by an insufficient pumping speed for hydrogen. As no temperature dependence is observed, a pronounced reversible interaction of hydrogen with O_γ can be excluded, too.

The Interaction of the Catalyst with Small Amounts of Methanol

As stated during the presentation of the TPD results, the applied oxygen pretreatment is found to be suitable for the formation of catalyst samples exposing O_γ without the simultaneous presence of O_α. Furthermore, samples exposing O_α without the presence of significant O_γ amounts can be obtained by adsorption of oxygen at lower temperatures. Therefore, pulse experiments over differently pretreated catalyst samples allow us to study the reactivity of the oxygen species O_γ and O_α without mutual interference. In addition, reference experiments are carried out over an oxygen-free catalyst. The formation of CO and CO_2 was not observed during these experiments; i.e., the decomposition and the total oxidation of methanol and formaldehyde did not occur to a detectable amount.

Figure 7a shows the responses of methanol and the product formaldehyde during methanol pulse experiments over an oxygen-free catalyst. The methanol response curves show comparable shapes and sizes for both temperatures. Furthermore, no significant amounts of formaldehyde or other products (not shown), such as carbon dioxide, carbon monoxide, water, or hydrogen, were detected. The observed small shift of the peak position toward shorter times at higher temperature can be rationalized by the temperature dependence of the mass transport by Knudsen diffusion. These results therefore indicate that methanol does not interact significantly with the oxygen-free catalyst.

The pulse responses for similar experiments over an oxygen-treated catalyst are displayed in Fig. 7b. In contrast to the experiments with the oxygen-free catalyst, reaction occurs on the oxygen-treated sample and the selective product formaldehyde is formed. Furthermore, a pronounced temperature dependence of the detected signals is visible; i.e., the methanol reactant response decreases and the formaldehyde product response increases at higher catalyst temperatures. This behavior can be attributed to the reaction of methanol with O_γ present on the oxygen-treated catalyst leading to the selective formation of formaldehyde. In addition, the results demonstrate that a significant formaldehyde formation induced by O_γ only takes place at temperatures above approximately 550 K. A comparison

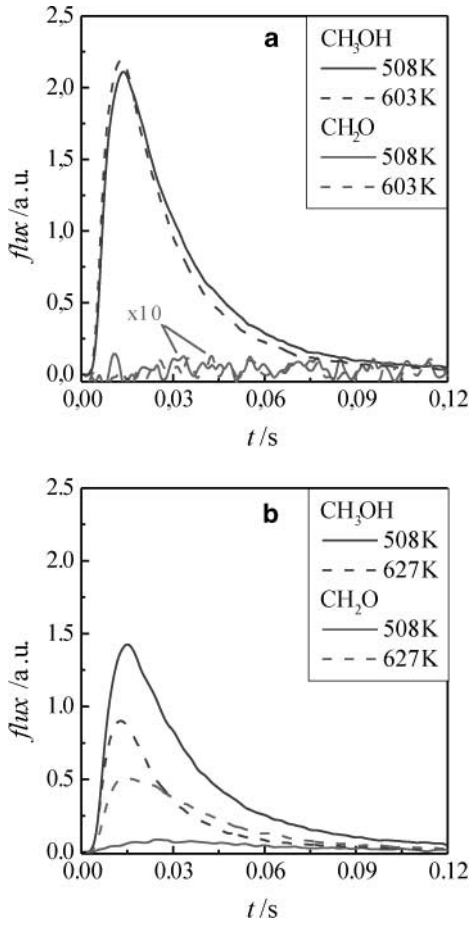

FIG. 7. Methanol and formaldehyde responses for pulses of 2.8×10^{14} molecules of a 1 : 10 methanol-in-neon mixture (a) at 508 and 603 K over an oxygen-free catalyst, and (b) at 508 and 627 K over an oxygen-treated catalyst.

of the methanol traces at 508 K in Figs. 7a and 7b shows a significantly smaller response for the oxygen-treated catalyst without a pronounced product formation, indicating irreversible adsorption of methanol within the short time scale of the pulse experiment. It must be noted that by using the same feed composition and by adjusting the size of the pulses to the same neon response, it was possible to dose the same amount of methanol reproducibly. Hence, the strongly differing results of experiments with the catalyst in the oxygen-free and oxygen-loaded state prove that adsorption and reaction of methanol only occur on oxygen-treated silver.

Figure 8 shows a time-resolved product distribution in terms of pulse responses of methanol, formaldehyde, water, and hydrogen during methanol pulse experiments over an oxygen-treated catalyst at different temperatures above 600 K. No significant responses were found for the unselective products carbon monoxide and carbon dioxide. Figure 8a displays the pulse responses at a catalyst temperature of 627 K as an effluent flux of each component

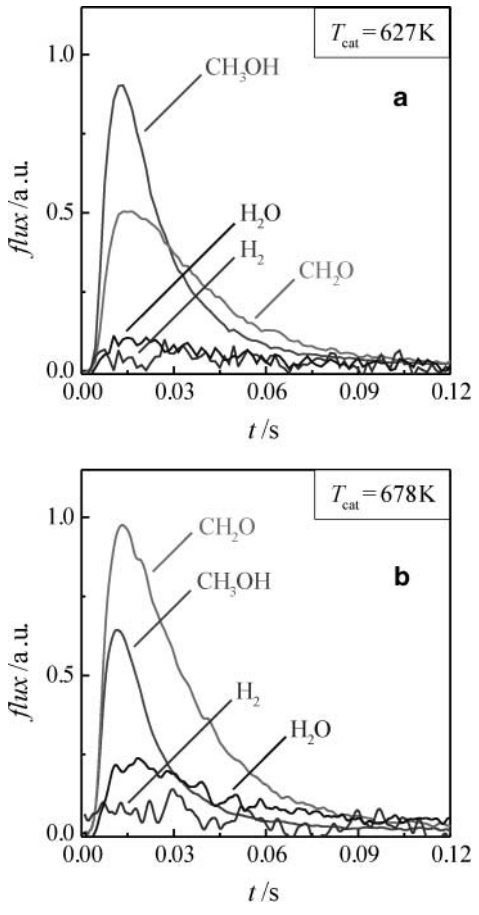

FIG. 8. Methanol, formaldehyde, water, and hydrogen responses for pulses of 2.8×10^{14} molecules of a 1 : 10 methanol-in-neon mixture over an oxygen-treated catalyst at (a) 627 K and (b) 678 K.

versus time after methanol introduction. Major responses are detected for unconverted methanol and the selectively formed product formaldehyde. However, a comparison of the pulse shapes shows that the formaldehyde response is significantly broadened, which is caused by a slow product formation after initial methanol adsorption. Furthermore, a small amount of water is detected as a broad signal parallel to the formaldehyde response, whereas no formation of hydrogen is observed. The response signals for similar pulse experiments at an increased catalyst temperature of 678 K are shown in Fig. 8b. In comparison to the experiment at lower temperature, an increased amount of formaldehyde and a decreased amount of methanol are detected within the pulse response, indicating an enhanced selective conversion of methanol to formaldehyde. In addition, an enlarged pulse-shaped formation of water is observed. However, no pronounced pulse responses are obtained for hydrogen, carbon monoxide, and carbon dioxide. Therefore, water can be identified as a primary gas-phase product of the selective methanol oxidation by O_γ.

For a comparison of the activity of the different oxygen species, further pulse experiments were conducted with a catalyst exposing the adsorbed oxygen species O_α. Therefore, the oxygen adsorption on the adsorbate-free catalyst was performed at 473 K, as described in the experimental section. A virtually complete O_α desorption is known to take place at a temperature of about 600 K (10, 23–27), restricting the experiments to a maximum catalyst temperature of 508 K.

Figure 9 shows the responses of methanol, formaldehyde, and carbon dioxide to methanol pulses at 508 K. Initially, a virtually complete conversion of methanol is found to occur, as shown in Fig. 9a. Furthermore, the formation of large amounts of carbon dioxide is observed, accompanied with only a minor formaldehyde production. However, a distinct change in the observed product distribution was found to take place upon the application of a large number of methanol pulses. This change can be attributed to a decrease in the coverage of O_α, as the oxidative product formation leads to a stoichiometric consumption of oxygen. Therefore, the decrease of the amount of adsorbed oxygen upon reaction with methanol was calculated. However, the exact oxygen coverage is not known, since the initial oxygen coverage is not known due to a slow desorption of oxygen

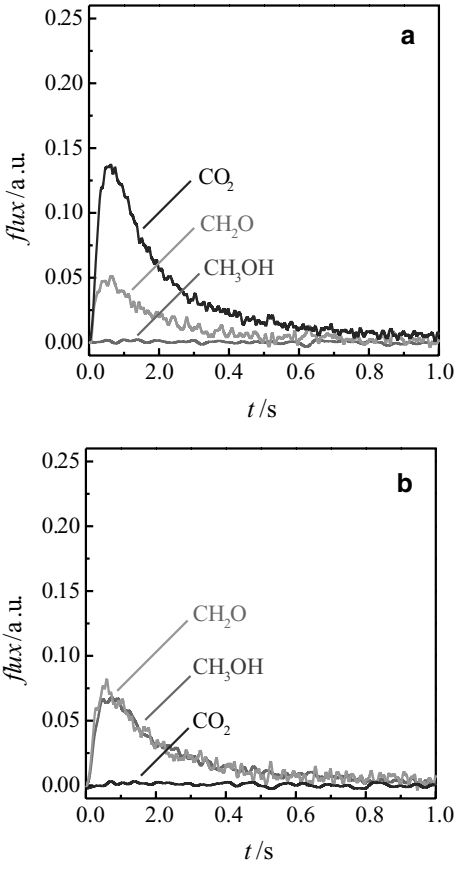

FIG. 9. Methanol, formaldehyde, and carbon dioxide responses for pulses of 7.5×10^{13} molecules of a 1 : 10 methanol-in-neon mixture at 508 K over a catalyst which was oxygen-treated at 473 K (a) at the beginning of the experiment and (b) after removal of 2.3×10^{15} oxygen atoms.

at reaction temperature. Figure 9b displays the pulse responses after the removal of 2.3×10^{15} oxygen atoms. In contrast to the initial findings, no formation of carbon dioxide is observed, and the production of formaldehyde is increased at an incomplete conversion of methanol. Hence, the overall selectivity toward the desired product formaldehyde is strongly enlarged at low coverages of O_α.

The Interaction of the Oxygen-Treated Catalyst with Higher Amounts of Methanol

The preceding pulse experiments were used to study the reactivity of the oxygen species O_γ and O_α toward methanol without mutual interference. Only a very small coverage of methanol-derived adsorbates was generated by pulsing methanol, which leads to the question of whether the obtained results are also relevant for reactions under atmospheric pressure. Higher and differently balanced reactant coverages can be present on the silver surface under industrial operation conditions. To achieve a higher coverage of methanol-derived intermediates, further experiments with continuous dosing of methanol were performed as flow experiments. In contrast to the pulse experiments in the Knudsen diffusion regime, the increased reactant pressure during these experiments may lead to the occurrence of additional intermolecular gas-phase reactions. Therefore, the reaction was carried out as a cyclic temperature-programmed experiment. During the initial heating ramp the catalytic performance of the oxygen-treated surface state is probed. The extent of gas-phase reactions is illustrated by the results obtained during the successive cooling ramp as the complete reduction of the catalyst at high temperatures leads to the formation of the inactive oxygen-free sample. Hysteresis phenomena between the heating and cooling branch can therefore be attributed to the catalytic reaction of methanol-derived intermediates at high coverages with O_γ.

Figure 10 displays the conversions and the product yields during a cyclic temperature-programmed reaction of a 1 : 10 methanol-in-neon mixture over an oxygen-treated catalyst up to 900 K using a heating ramp of 5 K min^{-1}. In contrast to the previously shown results from pulse experiments at comparable temperatures, a pronounced formation of carbon monoxide and hydrogen is observed during heating at temperatures above 600 K. The occurrence of gas-phase reactions during the successive cooling of the completely reduced and inactive catalyst leads to smaller yields. Reference experiments using inert quartz particles did not show any hysteresis and resulted in yields almost the same as those observed during the cooling ramp using Ag grains [20]. The resulting pronounced hysteresis in yields between the heating and the cooling branch therefore indicates that the initially observed formation of carbon monoxide and hydrogen is caused by the reaction of methanol with O_γ although homogeneous gas-phase reactions occur in parallel.

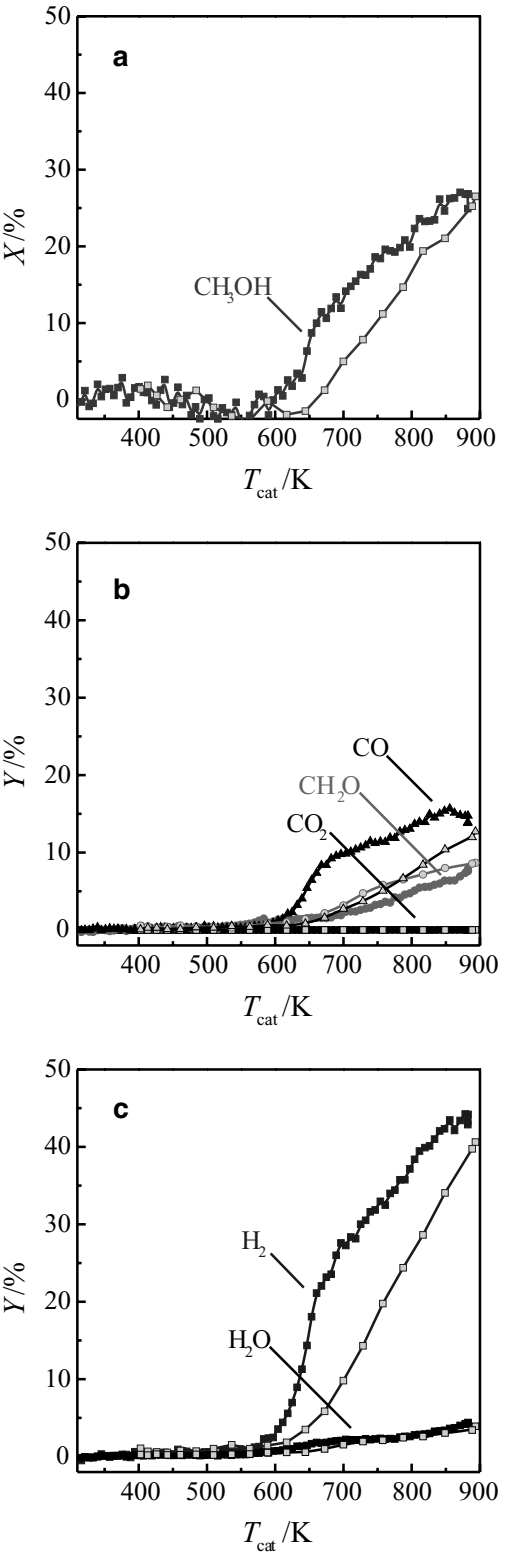

FIG. 10. Conversions (a) and yields (b, c) for the reaction of a 1 : 10 methanol-in-neon mixture over an oxygen-treated catalyst in the temperature range between 300 and 900 K. (solid symbols) The results during heating with 5 K min^{-1}; (open symbols) the extent of gas-phase reactions over the completely reduced and inactive catalyst during subsequent cooling.

Furthermore, only minor amounts of carbon dioxide and water are formed in both branches. The absence of a hysteresis in the yields for these products thus excludes a pronounced oxidation of hydrogen and carbon monoxide by O_γ, in agreement with the previous pulse experiments.

Additional flow experiments involving the codosing of methanol and oxygen were performed in order to obtain information on synergetic effects between O_α and O_γ. The experiments were carried out at constant reaction temperature over an initially oxygen-treated catalyst to ensure that the observed effects can be attributed to changes in the state of catalyst, particularly by the consumption of O_γ during the reaction. The occurrence of structural changes, as observed in previous studies at atmospheric pressure (8, 9), cannot be ruled out completely although a characterization of samples used under vacuum flow conditions via SEM micrographs (Fig. 1c) showed a much less pronounced formation of pin holes.

Figure 11 shows the conversions of methanol and oxygen (part a) and the yields of water, formaldehyde, carbon dioxide, and hydrogen (part b) for an isothermal flow experiment over an oxygen-treated catalyst at 585 K versus time on stream. The methanol-rich educt composition (methanol–oxygen ratio of 2.5) was chosen according to industrial conditions in which an understoichiometric amount of oxygen is used to achieve a maximum formaldehyde yield (1, 2, 29). During an initial period of 10 min on stream, almost constant conversions of methanol and oxygen were achieved. Furthermore, high yields of formaldehyde and water were obtained whereas only small amounts of carbon dioxide, carbon monoxide (trace not shown), and hydrogen were formed. After this initial period, a decline of the conversions and yields is observed, indicating a deactivation of the catalyst at 585 K.

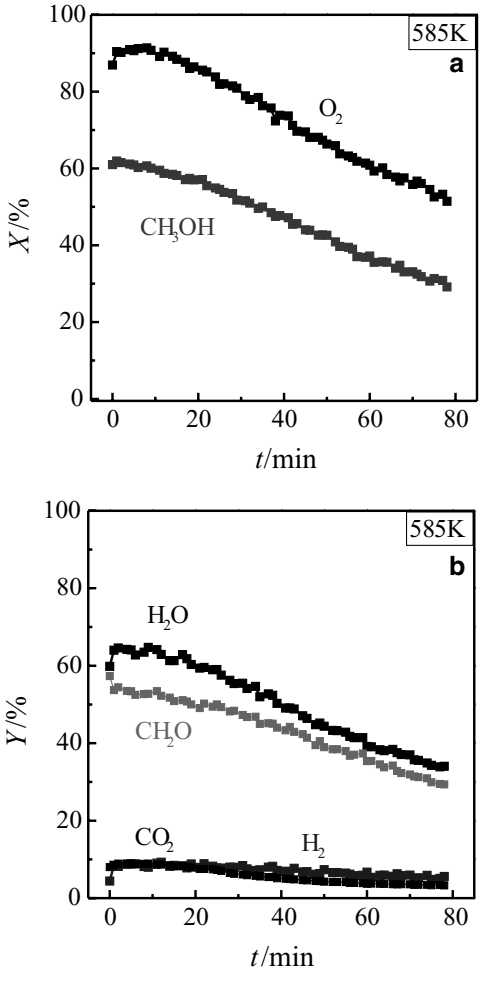

FIG. 11. Conversions (a) and yields (b) for the reaction of a 2.5 : 1 : 21 methanol- and oxygen-in-neon mixture over the oxygen-treated catalyst at 585 K.

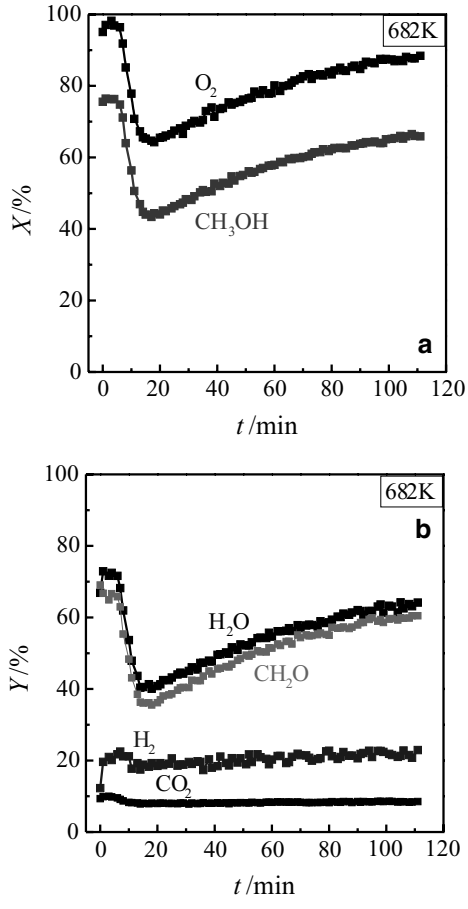

FIG. 12. Conversions (a) and yields (b) for the reaction of a 2.5 : 1 : 21 methanol- and oxygen-in-neon mixture over the oxygen-treated catalyst at 682 K.

The conversions of methanol and oxygen (part a) and the yields of water, formaldehyde, carbon dioxide, and hydrogen (part b) for a comparable isothermal flow experiment over an oxygen-treated catalyst at an increased cata temperature of 682 K are shown in Fig. 12. Within the first 6 min of operation, an almost complete conversion of oxygen and a high conversion of methanol were observed. In parallel, high formaldehyde and water yields are obtained within

this period. Afterward, a steep decrease in conversions occurred, leading to minimum values after about 18 min on stream. The respective yields of formaldehyde and water declined correspondingly, indicating a deactivation of the catalyst. However, after passing through the minimum in conversions and yields of formaldehyde and water a prolonged reactivation occurred. The formation of carbon dioxide and carbon monoxide (trace not shown) was rather small throughout the whole experiment. In addition, a small yield of hydrogen was observed. As discussed in the following, the reactivation is attributed to the reformation of O_γ from O_α via segregation of O_β at 682 K.

It is obvious that the formation of formaldehyde parallels the formation of water throughout all experiments. Thus, the conjecture that water is a primary gas-phase product based on the pulse experiments gains additional support. Furthermore, in contrast to pulse experiments over an oxygen-treated catalyst, a slight formation of hydrogen is observed under the flow conditions. Therefore, the formation of hydrogen appears to be enhanced in operations with increased amounts of reactants, leading to higher coverages.

4. DISCUSSION

The combination of different characterization techniques, pulse experiments after a suitable pretreatment specifically probing the reactivity of oxygen species without mutual interference, and flow experiments as complementary sources of information on the performance at higher coverage provides a deep insight into the reaction mechanism of the oxidation of methanol over the silver catalyst. In the following, the obtained results are discussed, leading to a consistent reaction scheme, shown in Fig. 13.

A comparison between the specific surface areas of the fresh and the used catalysts clearly showed the occurrence of sintering at high temperatures. A final specific surface area of 5.2×10^{-3} m^2 g^{-1} was determined for used catalysts. This result is in good agreement with specific surface areas of $3.0–7.0 \times 10^{-3}$ m^2 g^{-1} observed by Millar *et al.* (8, 30). The small specific surface area corresponding to about 10^{17} Ag surface atoms g^{-1} made it necessary to use very small pulse sizes of about 10^{14} molecules during catalytic experiments in order to avoid significant changes in the state of the catalyst during the experiment.

The SEM analysis was carried out to trace changes in surface morphology caused by the application of the chosen pretreatment procedures. In good agreement with results by Rhead and Mykura (15) and Bao *et al.* (16), the formation of strongly faceted silver surfaces is observed due to the oxygen pretreatment at high temperatures which is known to be caused by the formation of the O_γ species (16, 31). Therefore, the faceted surface which is macroscopically dull is strongly indicative of the presence of O_γ, in agreement with the TPD results. The reduction of the oxygen-treated catalyst with methanol during the preparation of the oxygen-free surface state led to the disappearance of the faceted surface structure. Therefore, it is safe to conclude that the reduction of the catalyst caused essentially complete destruction of the oxygen species O_γ.

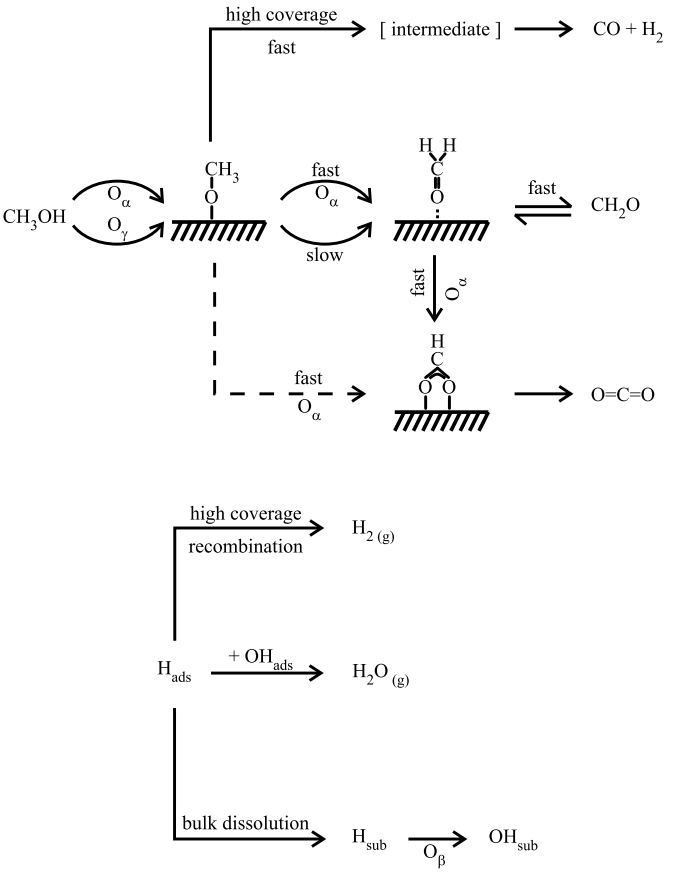

FIG. 13. Proposed reaction scheme of the oxidation of methanol silver catalysts.

Pulse experiments with oxygen indicated that the oxygen-treated state of the catalyst interacts only very weakly with gas-phase oxygen. The experiments allow us to conclude that the adsorption of gas-phase oxygen is strongly suppressed when O_γ is present. In contrast, an activated adsorption of oxygen is observed for corresponding experiments with the oxygen-free state of the catalyst. This behavior can be explained by the activated formation of the adsorbed atomic oxygen species O_α reported previously by several authors (10, 23–27). The adsorption was found to occur at least partly irreversibly within the short time scale of TAP pulse experiments. This observation might, on one hand, be explained by the low, hardly traceable rate of an associative desorption process at the low coverage generated during an pulse experiment. On the other hand, the dissolution of oxygen and the formation of O_β cannot be excluded. In this way, the presence of O_γ is beneficial for a high selectivity to formaldehyde since the formation of

the less selective species, O_α, is strongly suppressed, resulting in a lower coverage of O_α under steady-state reaction conditions.

The pulse experiments over the oxygen-treated catalyst proved that carbon monoxide does not show a pronounced interaction with O_γ under the applied pulse conditions. Furthermore, no significant conversion and no carbon dioxide formation were observed:

$$CO + O_\gamma \nrightarrow CO_2. \qquad [3]$$

Thus, O_γ shows a significantly different behavior compared to O_α, which is known to oxidize carbon monoxide in a "clean-off" reaction (32). Thus, the formation of carbon dioxide observed in other experiments cannot be explained by the oxidation of carbon monoxide by O_γ. Additional support for this conjecture is obtained from the temperature-programmed flow experiments using a methanol in neon mixture over an oxygen-treated catalyst. Despite the presence of O_γ, carbon monoxide was formed as major product and no pronounced formation of carbon dioxide was observed.

Further pulse experiments were carried out with hydrogen. Due to the fact that the detection of hydrogen is complicated by pumping effects (28), broadened and oversized pulse responses were obtained. However, it is safe to conclude that no hydrogen conversion took place, as no significant temperature dependence of the calculated conversions was found within the investigated temperature range:

$$H_2 + O_\gamma \nrightarrow H_2O. \qquad [4]$$

Therefore, the formation of water during pulse experiments over an oxygen-treated catalyst cannot be explained by a secondary oxidation of gas-phase hydrogen. The formation of hydrogen as a major product during the temperature-programmed flow experiment with a methanol-in-neon mixture over an oxygen-treated catalyst supports this conjecture: a pronounced oxidation of hydrogen by O_γ was not observed. This result is also in good agreement with the results obtained in H_2 TPSR studies by Schubert *et al.* (18). The authors used a silver sample exposing all oxygen species and concluded from the temperature dependence of the water formation that the species O_γ did not react with hydrogen.

Methanol pulse experiments over an oxygen-free catalyst showed neither a significant conversion nor a reversible interaction with the catalyst. The observed inertness of a clean silver surface is in good agreement with previous studies (5, 6, 33). In contrast, a catalyst exposing either O_α or O_γ was found to be highly active for the conversion of methanol. O_γ induces a strong adsorption of methanol on the catalyst surface without a pronounced further reaction in the temperature range below 550 K. Therefore, the presence of these oxygen species is considered essential for the adsorption of methanol yielding adsorbed methoxy species and hydroxyl groups:

$$CH_3OH_{(g)} + O_\gamma/O_\alpha \rightarrow CH_3O_{(ads)} + OH_{(ads)}. \qquad [5]$$

This result is in good agreement with early results obtained by Wachs and Madix (5), Bhattacharyya *et al.* (33), and Bao and Deng (6).

In contrast to previous studies, our temporal-analysis-of-products approach allowed us to investigate the reactivity of the different oxygen species at constant temperature under variations of coverage. In good agreement with recent reports on the catalytic behavior of the O_γ species, pulse experiments proved the high selectivity of this oxygen species toward the formation of formaldehyde when an understoichiometric amount of methanol was dosed. Furthermore, water was found to be a primary gas-phase product of the selective oxidation of methanol with O_γ, since formaldehyde and water showed almost parallel responses to methanol pulses:

$$\begin{aligned} CH_3OH_{(g)} + O_\gamma &\rightarrow CH_3O_{(ads)} + OH_{(ads)} \\ &\rightarrow CH_2O_{(g)} + H_2O_{(g)}. \end{aligned} \qquad [6]$$

As expected, enlarging methanol conversion by increasing the reaction temperature resulted in a parallel rise in the yields of formaldehyde and water. In addition, the simultaneous formation of water and formaldehyde under all applied conditions during flow experiments with an oxygen-in-neon mixture confirmed the results from the pulse experiments and is therefore another piece of evidence that both gas-phase products are formed within the same primary reaction step.

However, this conjecture is in contrast to previous reports stating that hydrogen is a primary gas-phase product of the selective oxidation of methanol by O_γ (18). These studies may have been impaired by the simultaneous participation of different oxygen species in the reaction. Furthermore, under reaction conditions where the surface is not predominantly covered with O_γ the formation of adsorbed atomic hydrogen might take place by the thermal decomposition of the methoxy species. Thus, gas-phase hydrogen can be formed by associative desorption, as observed during the experiments with a continuous reactant feed. In the case of the pulse experiments the formation of hydrogen may be underestimated, as the dissolution of adsorbed hydrogen atoms into the silver bulk cannot be excluded.

The conjecture that water is a primary product of the selective oxidation of methanol by O_γ implies that the catalyst is reduced during reaction. Thus, the O_γ-based catalytic activity can only be maintained when the regeneration of this species occurs at a sufficient rate. During the flow experiments with codosed methanol and oxygen at constant reaction temperature, the regeneration of O_γ was prevented

by the lower reaction temperature of 585 K leading to a deactivation of the catalyst. However, at an increased reaction temperature of 682 K the deactivation of the catalyst was followed by a slow reactivation, which can be rationalized by the regeneration of O_γ:

$$0.5O_{2(g)} \rightarrow O_\alpha \rightarrow O_\beta \rightarrow O_\gamma. \quad [7]$$

Obviously, the catalytic behavior of the silver-oxygen redox system resembles the Mars–van Krevelen mechanism over oxide catalysts since the dehydrogenation step involves lattice-bound oxygen (O_γ) replenished from the bulk (O_β), which, in turn, originates from the separately occurring dissolution of adsorbed atomic oxygen (O_α) (34). Thus, the reaction mechanism over silver catalysts is closely related to oxidative dehydrogenation over ferric molybdate (35).

In agreement with previous reports, O_α was found to oxidize methanol with a very limited selectivity toward formaldehyde at high coverage:

$$CH_3OH + 3O_\alpha \rightarrow CO_2 + 2H_2O;\ \Theta_{O_\alpha} \approx 1. \quad [8]$$

However, by lowering the coverage a distinct shift in selectivity was observed and a very high selectivity toward formaldehyde (exceeding 90%) was found:

$$CH_3OH + O_\alpha \rightarrow CH_2O + H_2O;\ 1 \gg \Theta_{O_\alpha} \geq 0. \quad [9]$$

As the experiments were carried out at 508 K and O_γ was shown to cause a significant product formation only above 550 K, an interference by this oxygen species can be safely excluded.

Finally, the results of continuous-flow experiments with methanol over an oxygen-treated catalyst indicate a limited selectivity when a high coverage of the methoxy species is reached, which decomposes forming hydrogen and carbon monoxide:

$$2CH_3O_{(ads)} \rightarrow 2CO_{(g)} + 3H_{2(g)}. \quad [10]$$

Therefore, the performance of the catalyst is significantly enhanced by the presence of small amounts of O_α, which cause a rapid reaction of the methoxy species to formaldehyde, thus lowering their coverage.

The proposed reaction scheme is summarized in Fig. 13. Both oxygen species induce the dissociative chemisorption of methanol, leading to the formation of adsorbed methoxy species. In contrast to O_γ, O_α causes further reactions, which include breaking the C–H bond, yielding the desired product formaldehyde. However, O_α is also involved in the deep oxidation of primarily formed formaldehyde, thus dramatically lowering the selectivity at higher coverages of O_α. Contrary to O_α, it is assumed that O_γ is able to break only the O–H bond, not the C–H bond. At reaction temperatures above 550 K, the adsorbed methoxy species decomposes in a consecutive step into formaldehyde. Adsorbed atomic hydrogen may either recombine, yielding gas-phase hydrogen at high coverages, or it may react with OH groups, forming water. It may also dissolve in the bulk of the catalyst, where it can react with O_β (16).

5. CONCLUSIONS

1. Methanol pulse experiments over an oxygen-treated catalyst exclusively exposing the high-temperature species O_γ provided evidence that this oxygen species causes the highly selective oxidative dehydrogenation of methanol to formaldehyde at temperatures above 550 K.

2. A comparison of the pulse response shapes for formaldehyde, water, and hydrogen shows that water is a primary gas-phase product and that only small amounts of hydrogen are formed.

3. The identification of water as a primary gas-phase product implies that the lattice-bound surface oxygen species O_γ is consumed during the reaction. O_γ is replenished by segregation of bulk-dissolved atomic oxygen (O_β), which, in turn, originates from the separately occurring dissolution of adsorbed atomic oxygen (O_α). Thus, the reaction mechanism over silver is closely related to the Mars–van Krevelen mechanism over ferric molybdate.

4. In contrast, the low-temperature oxygen species O_α was found to be highly active, leading to total oxidation at high coverages. However, at low coverages O_α also causes the selective formation of formaldehyde.

5. The presence of O_γ on the silver surface is therefore decisive for the high selectivity to formaldehyde for two reasons: it acts as a selective reactant, only breaking O–H bonds, and it lowers the coverage of O_α.

ACKNOWLEDGMENTS

The authors gratefully acknowledge financial support by the Deutsche Forschungsgemeinschaft (HI 716/1-3) and Fonds der Chemischen Industrie (FCI).

REFERENCES

1. Twigg, M. V., *in* "Catalyst Handbook" (M. V. Twigg, Ed.), 2nd ed., p. 490. Manson Publishing, London, 1996.
2. Weissermel, K., and Arpe, H.-J., "Industrielle Organische Chemie," 4th ed., p. 40. Wiley–VCH, New York, 1998.
3. Sperber, H., *Chem.-Ing.-Tech.* **41**, 962 (1969).
4. Reuss, G., Disteldorf, W., Grundler, O., and Hilt, A., *in* "Ullmann's Encyclopedia of Industrial Chemistry" (W. Gerhartz, Ed.), 5th ed., Vol. A11 p. 619. Verlag Chemie, Weinheim, 1988.
5. Wachs, I. E., and Madix, R. J., *Surf. Sci.* **76**, 531 (1978).
6. Bao, X., and Deng, J., *J. Catal.* **99**, 391 (1986).
7. Lefferts, L., van Ommen, J. G., and Ross, J. R. H., *Appl. Catal.* **23**, 385 (1986).
8. Millar, G. J., Nelson, M. L., and Uwins, P. J. R., *J. Catal.* **169**, 143 (1997).
9. Nagy, A., Mestl, G., Rühle, T., Weinberg, G., and Schlögl, R., *J. Catal.* **179**, 548 (1998).

10. Campbell, C. T., *Surf. Sci.* **157**, 43 (1985).
11. Bao, X., Muhler, M., Pettinger, B., Schlögl, R., and Ertl, G., *Catal. Lett.* **22**, 215 (1993).
12. Bao, X., Muhler, M., Schedel-Niedrig, T., and Schlögl, R., *Phys. Rev. B* **54**, 2249 (1996).
13. Salanov, A. N., and Savchenko, V. I., *React. Kinet. Catal. Lett.* **61**, 323 (1997).
14. Boronin, A. I., Koscheev, S. V., and Zhidomirov, G. M., *J. Electron Spectrosc. Relat. Phenom.* **96**, 43 (1998).
15. Rhead, G. E., and Mykura, H., *Acta Metall.* **10**, 843 (1962).
16. Bao, X., Lehmpfuhl, G., Weinberg, G., Schlögl, R., and Ertl, G., *J. Chem. Soc. Faraday Trans.* **88**, 865 (1992).
17. Herein, D., Nagy, A., Schubert, H., Weinberg, G., Kitzelmann, E., and Schlögl, R., *Z. Phys. Chem.* **197**, 67 (1996).
18. Schubert, H., Tegtmeyer, U., and Schlögl, R., *Catal. Lett.* **28**, 383 (1994).
19. Gleaves, J. T., Ebner, J. R., and Kuechler, T. C., *Catal. Rev.-Sci. Eng.* **30**(1), 49 (1988).
20. van Veen, A. C., Zanthoff, H. W., Hinrichsen, O., and Muhler, M., *J. Vac. Sci. Technol. A* **19**, 651 (2001).
21. Bao, X., Muhler, M., Pettinger, B., Uchida, Y., Lehmpfuhl, G., Schlögl, R., and Ertl, G., *Catal. Lett.* **32**, 171 (1995).
22. Rigas, N. C., Svoboda, G. D., and Gleaves, J. T., *in* "Catalytic Selective Oxidation" (S. T. Oyama and J. W. Hightower, Eds.), p. 183. Am. Chem. Soc., Washington, DC, 1993.
23. Rovida, G., and Pratesi, F., *Surf. Sci.* **52**, 542 (1975).
24. Engelhardt, H. A., and Menzel, D., *Surf. Sci.* **57**, 591 (1976).
25. Backx, C., de Groot, C. P. M., and Biloen, P., *Surf. Sci.* **104**, 300 (1981).
26. Campbell, C. T., and Paffett, M. T., *Surf. Sci.* **143**, 517 (1984).
27. Bowker, M., Barteau, M. A., and Madix, R. J., *Surf. Sci.* **92**, 528 (1980).
28. Rothaemel, M., Ph.D. thesis. Ruhr-Universität Bochum, 1995.
29. Cao, Y., Dai, W.-L., and Deng, J.-F., *Appl. Catal. A* **158**, L27 (1997).
30. Millar, G. J., Metson, J. B., Bowmaker, G. A., and Cooney, R. P., *J. Chem. Soc. Faraday Trans.* **91**, 4149 (1995).
31. Bao, X., Pettinger, B., Ertl, G., and Schlögl, R., *Ber. Bunsen-Ges. Phys. Chem.* **97**, 322 (1993).
32. Engelhardt, H. A., Bradshaw, A. M., and Menzel, D., *Surf. Sci.* **40**, 410 (1973).
33. Bhattacharyya, S. K., Nag, N. K., and Ganguly, N. D., *J. Catal.* **23**, 158 (1971).
34. Mars, P., and van Krevelen, D. W., *Chem. Eng. Sci. Suppl.* **3**, 41 (1954).
35. Muhler, M., *in* "Handbook of Heterogeneous Catalysis" (G. Ertl, H. Knözinger, and J. Weitkamp, Eds.), Vol. 5, p. 2274. Verlag Chemie, Weinheim, 1997.